High-Q lithium niobate microdisk resonators on a chip for efficient electro-optic modulation

Jie Wang,[1] Fang Bo,[1,*] Shuai Wan,[1] Wuxia Li,[2] Feng Gao,[1] Junjie Li,[2] Guoquan Zhang,[1,3] and Jingjun Xu[1]

[1]*The MOE Key Laboratory of Weak Light Nonlinear Photonics, TEDA Applied Physics Institute and School of Physics, Nankai University, Tianjin 300457, China*
[2]*Beijing National Laboratory for Condensed Matter Physics, Institute of Physics, Chinese Academy of Sciences, Beijing 100080, China*
[3]*zhanggq@nankai.edu.cn*
[*]*bofang@nankai.edu.cn*

Abstract: Lithium niobate (LN) microdisk resonators on a LN-silica-LN chip were fabricated using only conventional semiconductor fabrication processes. The quality factor of the LN resonator with a 39.6-μm radius and a 0.5-μm thickness is up to 1.19×10^6, which doubles the record of the quality factor 4.84×10^5 of LN resonators produced by microfabrication methods allowing batch production. Electro-optic modulation with an effective resonance-frequency tuning rate of 3.0 GHz/V was demonstrated in the fabricated LN microdisk resonator.

OCIS codes: (130.3730) Lithium niobate; (130.3990) Micro-optical devices; (230.3120) Integrated optics devices; (230.5750) Resonators.

References and links

1. L. Arizmendi, "Photonic applications of lithium niobate crystals," Phys. Status Solidi A **201**, 253-283 (2004).
2. V. S. Ilchenko, A. B. Matsko, A. A. Savchenkov, and L. Maleki, "Low-threshold parametric nonlinear optics with quasi-phase-matched whispering-gallery modes," J. Opt. Soc. Am. B **20**, 1304-1308 (2003).
3. V. S. Ilchenko, A. A. Savchenkov, A. B. Matsko, and L. Maleki, "Nonlinear optics and crystalline whispering gallery mode cavities," Phys. Rev. Lett. **92**, 043903 (2004).
4. K. Sasagawa and M. Tsuchiya, "Highly efficient third harmonic generation in a periodically poled MgO:$LiNbO_3$ disk resonator," Appl. Phys. Express **2**, 122401 (2009).
5. J. U. Furst, D. V. Strekalov, D. Elser, A. Aiello, U. L. Andersen, C. Marquardt, and G. Leuchs, "Low-threshold optical parametric oscillations in a whispering gallery mode resonator," Phys. Rev. Lett. **105**, 263904 (2010).
6. J. U. Furst, D. V. Strekalov, D. Elser, M. Lassen, U. L. Andersen, C. Marquardt, and G. Leuchs, "Naturally phase-matched second-harmonic generation in a whispering-gallery-mode resonator," Phys. Rev. Lett. **104**, 153901 (2010).
7. T. Beckmann, H. Linnenbank, H. Steigerwald, B. Sturman, D. Haertle, K. Buse, and I. Breunig, "Highly tunable low-threshold optical parametric oscillation in radially poled whispering gallery resonators," Phys. Rev. Lett. **106**, 143903 (2011).
8. T.-J. Wang, J.-Y. He, C.-A. Lee, and H. Niu, "High-quality $LiNbO_3$ microdisk resonators by undercut etching and surface tension reshaping," Opt. Express **20**, 28119-28124 (2012).
9. C. Wang, M. J. Burek, Z. Lin, H. A. Atikian, V. Venkataraman, I. C. Huang, P. Stark, and M. Loncar, "Integrated high quality factor lithium niobate microdisk resonators," Opt. Express **22**, 30924-30933 (2014).
10. R. Wang and S. A. Bhave, "Free-standing high quality factor thin-film lithium niobate micro-photonic disk resonators," arXiv:1409.6351 (2014).
11. J. Lin, Y. Xu, Z. Fang, M. Wang, J. Song, N. Wang, L. Qiao, W. Fang, and Y. Cheng, "Fabrication of high-Q lithium niobate microresonators using femtosecond laser micromachining," Sci. Rep. **5**, 8072 (2015).

#246339 Received 20 Jul 2015; revised 17 Aug 2015; accepted 18 Aug 2015; published 24 Aug 2015

12. A. Guarino, G. Poberaj, D. Rezzonico, R. Degl'Innocenti, and P. Guenter, "Electro-optically tunable microring resonators in lithium niobate," Nat. Photonics **1**, 407-410 (2007).
13. C. Y. J. Ying, C. L. Sones, A. C. Peacock, F. Johann, E. Soergel, R. W. Eason, M. N. Zervas, and S. Mailis, "Ultra-smooth lithium niobate photonic micro-structures by surface tension reshaping," Opt. Express **18**, 11508-11513 (2010).
14. M. Levy, R. M. Osgood, R. Liu, L. E. Cross, G. S. Cargill, A. Kumar, and H. Bakhru, "Fabrication of single-crystal lithium niobate films by crystal ion slicing," Appl. Phys. Lett. **73**, 2293-2295 (1998).
15. F. Bo, S. H. Huang, S. K. Ozdemir, G. Zhang, J. Xu, and L. Yang, "Inverted-wedge silica resonators for controlled and stable coupling," Opt. Lett. **39**, 1841-1844 (2014).
16. M. Oxborrow, "Traceable 2-D finite-element simulation of the whispering-gallery modes of axisymmetric electromagnetic resonators," IEEE Trans. Microwave Theory Tech. **55**, 1209-1218 (2007).
17. T.-J. Wang, C.-H. Chu, and C.-Y. Lin, "Electro-optically tunable microring resonators on lithium niobate," Opt. Lett. **32**, 2777-2779 (2007).
18. Q. Xu, B. Schmidt, S. Pradhan, and M. Lipson, "Micrometre-scale silicon electro-optic modulator," Nature **435**, 325-327 (2005).
19. L. Zhou and A. W. Poon, "Silicon electro-optic modulators using p-i-n diodes embedded 10-micron-diameter microdisk resonators," Opt. Express **14**, 6851-6857 (2006).
20. P. Dong, S. Liao, H. Liang, W. Qian, X. Wang, R. Shafiiha, D. Feng, G. Li, X. Zheng, A. V. Krishnamoorthy, and M. Asghari, "High-speed and "silicon modulator based on a racetrack resonator with a 1 V drive voltage," Opt. Lett. **35**, 3246-3248 (2010).
21. J. Zhu, S. K. Ozdemir, Y.-F. Xiao, L. Li, L. He, D.-R. Chen, and L. Yang, "On-chip single nanoparticle detection and sizing by mode splitting in an ultrahigh-Q microresonator," Nat. Photonics **4**, 46-49 (2010).
22. L. He, S. K. Ozdemir, J. Zhu, W. Kim, and L. Yang, "Detecting single viruses and nanoparticles using whispering gallery microlasers," Nat. Nanotechnol. **6**, 428-432 (2011).
23. L. Shao, X. F. Jiang, X. C. Yu, B. B. Li, W. R. Clements, F. Vollmer, W. Wang, Y. F. Xiao, and Q. Gong, "Detection of single nanoparticles and lentiviruses using microcavity resonance broadening," Adv. Mater. **25**, 5616-5620 (2013).
24. S. K. Ozdemir, J. Zhu, X. Yang, B. Peng, H. Yilmaz, L. He, F. Monifi, S. H. Huang, G. L. Long, and L. Yang, "Highly sensitive detection of nanoparticles with a self-referenced and self-heterodyned whispering-gallery Raman microlaser," P. Natl. Acad. Sci. USA. **111**, E3836-E3844 (2014).
25. L. He, S. K. Ozdemir, and L. Yang, "Whispering gallery microcavity lasers," Laser Photonics Rev. **7**, 60-82 (2013).
26. B. Peng, S. K. Ozdemir, F. Lei, F. Monifi, M. Gianfreda, G. L. Long, S. Fan, F. Nori, C. M. Bender, and L. Yang, "Parity-time-symmetric whispering-gallery microcavities," Nat. Phys. **10**, 394-398 (2014).
27. B. Peng, S. K. Ozdemir, S. Rotter, H. Yilmaz, M. Liertzer, F. Monifi, C. M. Bender, F. Nori, and L. Yang, "Loss-induced suppression and revival of lasing," Science **346**, 328-332 (2014).
28. B. Peng, S. K. Ozdemir, W. Chen, F. Nori, and L. Yang, "What is and what is not electromagnetically induced transparency in whispering-gallery microcavities," Nat. Commun. **5**, 5082 (2014).

1. Introduction

Lithium niobate (LN) is referred to as photonic silicon for its extraordinary electro-optic (r_{33} = 30.9 pm/V), nonlinear optical (d_{33} =41.7 pm/V), and acousto-optic effects in a wide wavelength band ranging from 0.35 μm to 5 μm [1]. It is widely used in optical, electro-optic and acousto-optic devices such as electro-optic modulator, wavelength convertor, and surface acoustic wave filter. Recently, whispering gallery mode (WGM) resonators made from LN crystal [2–11] have been attracting much attention due to the combination of high quality (Q) factor, resonance in a very broad band, tunable coupling features of WGM resonators and excellent properties of LN crystal itself. Highly tunable nonlinear optical devices that operate with remarkably low turn-on powers down to mW were successfully demonstrated in millimeter-size LN WGM resonators with Q factor on the order of 10^7 fabricated by traditional optical fabrication techniques such as cutting and polishing [2–7]. Electrically tunable filter with wavelength tuning rate of 0.14 GHz/V was realized in a micrometer-size LN ring resonator based on the electro-optic effect of LN crystal [12]. The quality factor of the above mentioned ring resonator is only 10^4, which is mainly limited by the scattering of light from the rough surface of the ring waveguide.

Actually, the mass fabrication of an integrated optical device of LN, especially WGM resonators that have a undercut structure, has always been a challenging task due to the strong

#246339 Received 20 Jul 2015; revised 17 Aug 2015; accepted 18 Aug 2015; published 24 Aug 2015

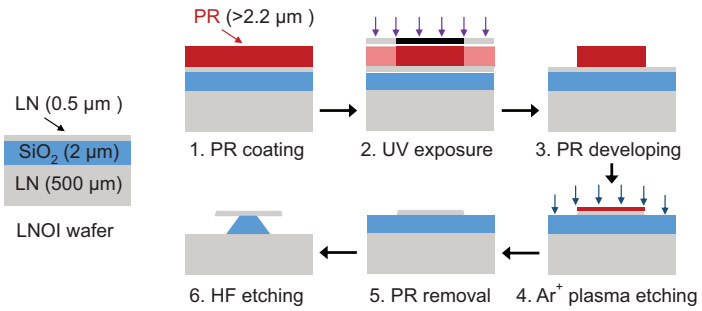

Fig. 1. Structure of LNOI wafer and the schematic diagram of the process to fabricate LN microdisk resonators. PR: photoresist; HF: hydrofluoric acid.

etching resistance of LN crystal. Even the etching rate of the -C face of LN is faster than that of X, Y and +C faces, it is only several nanometers per minute with the concentrated or diluted HF (or HF: HNO3) at room temperature. Introduction of structural defects by ion implantation and excimer laser ablation can accelerate the etching rate of LN considerably. By using He^+ implantation assisted HF etching, LN microdisks with an undercut structure was fabricated on -C face of a bulk LN crystal [8]. During the HF etching process, the exposed part of the -C face with faster etching rate was first etched down to the He^+ resident layer, and then the layer having introduced defects was etched downward and laterally, resulting in an undercut structure. Although a high temperature annealing technique [13] was used to smooth the surface of the resonator, the Q factor was only 2.6×10^4 [8].

Compared with wet etching methods, dry etching processes, i.e. reactive ion etching (RIE), may be a better method to fabricate integrated device on LN because of their relatively high etching rates of a few tens of nanometers per minute. Unfortunately, no undercut structure including WGM resonators can be obtained from bulk LN crystal. Recently, LN film on silicon sample and LN film on insulators (LNOI) wafer that has a sandwich structure with a layer of silica lying between a thin LN film and a thick LN substrate were prepared by using ion slicing and bonding techniques [14]. Benefiting from the preparations of these LN films, LN WGM resonators with micrometer size and Q up to 4.84×10^5 were produced by using RIE to etch LN and HF/XeF_2 to etch silica/silicon thereby fabricating a pillar [9, 10]. LN WGM resonators on LNOI wafer with micrometer size and Q factor of 10^5 were also made using femtosecond laser micromachining [11], followed by focused ion beam polishing and then high temperature annealing, which however does not allow batch production.

In this work, high-Q monocrystalline LN WGM resonators were fabricated on a LNOI wafer by using UV-photolithography, Ar^+ plasma etching, and HF etching. The measured Q factor in 1550 nm band of LN resonators with a radius of 39.6 μm and a thickness of 500 nm are up to 1.19×10^6, which is more than two times larger than the reported highest Q factor 4.84×10^5 for a on-chip LN WGM resonator [10]. Electro-optic modulation at 1550 nm was demonstrated by applying an alternating voltage along the c axis of LN crystal. Thanks to extraordinary electro-optic effect of LN crystal, we observed a 3.0-GHz/V tuning rate of the resonance frequency of LN WGM resonators.

2. Fabrication methods

Microdisk resonators were fabricated on a LN-silica-LN wafer prepared (by NANOLN) by using ion slicing and wafer bonding techniques [14]. The thicknesses of the LN thin film functioning as device layer, the buried silica layer, and the LN support layer of the LNOI wafer were

#246339 Received 20 Jul 2015; revised 17 Aug 2015; accepted 18 Aug 2015; published 24 Aug 2015

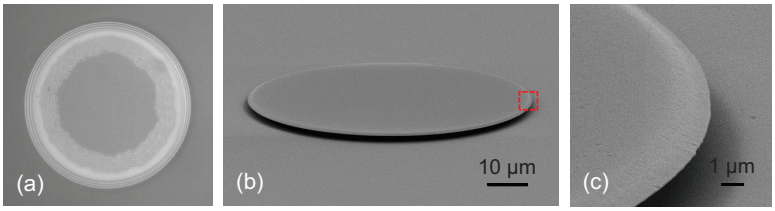

Fig. 2. Microscope images of a LN microdisk resonator with an external radius of 39.6 μm. (a) Optical microscope image showing the top view of the LN microdisk. (b) and (c): Scanning electron microscope images showing the oblique views of the whole and the edge (labeled by the red square) of the LN microdisk, respectively.

0.5 μm, 2 μm, and 500 μm, respectively. The fabrication process involved three main steps: UV-lithography, Ar^+ plasma etching, and HF etching. The processing details are schematically illustrated in Fig. 1. Firstly, a layer of photoresist was prepared on the LNOI sample by spin coating method, then disk-shaped photoresist pads, which serves as the Ar^+ plasma etching mask, were transfered from a photomask onto the top of the LNOI sample using UV-lithography. Thereafter, the LN device layer was etched by Ar^+ plasma in a RIE system. The ratio of the etching rates of the photoresist and LN crystal is about 4:1. Accordingly, the photoresist pad with thickness greater than 2.2 μm was employed in our experiments to provide well protection for the LN film underneath photoresist pads during the entire Ar^+ plasma etching process. In this case, the exposed part of the 500-nm thick LN device layer was totally removed, while the other part covered by the photoresist was well protected, thus the finely polished top surface of the LN film was maintained. After the residuary photoresist was removed by using acetone, HF was employed to etch the silica layer from the edge to the center of the LN disk at room temperature for about 15 minutes to form the undercut pillar. Although the LN film was also slightly etched by HF during this process, the smooth surface of the LN film was still kept due to the dramatically low etching rate of LN crystal especially when compared with that of silica, which was further confirmed by the microimages and the measured Q factors up to 10^6 of the fabricated LN microdisk resonators.

3. Characteristics of LN resonators

The fabricated LN microdisk resonators were first characterized using optical microscope and scanning electron microscope techniques. The optical microscope image of a LN resoantor with a radius of 39.6 μm is shown in Fig. 2(a). This resonator was produced by using a UV-lithography mask with opaque rounds of a radius of 40 μm, which verified that our processing method is suitable to fabricate microresonators with given size and shape for the absence of postprocessing that may change the size of resonator, such as high-temperature annealing and CO_2 laser reflow. A series of concentric circles originated from equal thickness interference were clearly observed from Fig. 2(a). The innermost dark circle with an irregular border reveals the top surface of the silica pillar. The bright and dark irregular patterns appeared alternatively just outside the innermost dark circle indicate an inclined and matte side surface of the silica pillar. The outermost ring with a nearly perfect circle shape shows the boundary of the resonator. The equidistant circular dark and bright rings including the outermost ring tell us that the fabricated LN microdisk resonator has a wedge shape, and more importantly, it has a smooth side surface. Such a smooth inclined side surface helps one to get a high Q factor and was further verified by the scanning electronic microscope (SEM) images shown in Figs. 2(b) and 2(c), from which we can clearly see the nice surface of the fabricated LN microdisk. The

#246339 Received 20 Jul 2015; revised 17 Aug 2015; accepted 18 Aug 2015; published 24 Aug 2015

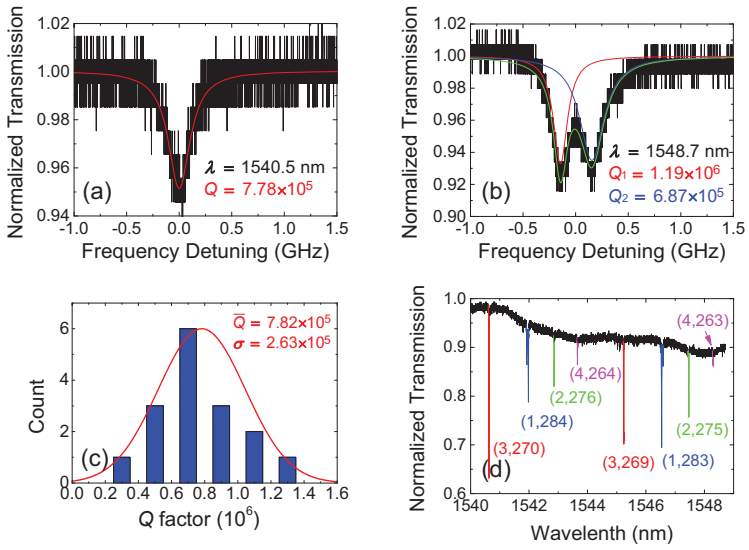

Fig. 3. Transmission spectra and the measured Q factors. (a) and (b): Normalized transmission spectra with one and two dips showing Q factors of 7.78×10^5 and 1.19×10^6, respectively. (c) Histogram showing the statistic result of 16 LN resonators from two samples fabricated in a batch. Mean ($\bar{Q}$) and standard deviation (σ) of Q factors are 7.82×10^5 and 2.63×10^5, respectively. (d) Broad band transmission spectrum showing free spectrum ranges and the assigned modes. All the efficiently coupled modes are $TE_{m,n}$ modes, where m and n indicate the radial and azimuthal mode numbers.

undercut feature of the LN resonator is demonstrated as well by the SEM pictures. We noticed that the width of the wedge of the microdisk might be different for LN resonators on different chips. In order to show the interference pattern demonstrating the wedge more clearly, the optical microscope image of a LN resonator with a relatively broad wedge is demonstrated in Fig. 2(a). This resonator is not the same one as that shown in Figs. 2(b) and 2(c).

To characterize the optical properties of the fabricated LN WGM resonator, the transmission spectra of the resonator coupled with a tapered fiber were measured by using a tunable laser in communication band near 1550 nm. The experimental setup is similar to that used in our previous paper [15]. Figures 3(a) and 3(b) show normalized transmission spectra measured in deep under coupling regime using low light power to avoid thermal effect. In this case, the measured Q factor is approximately equal to the intrinsic Q factor of the resonator. The Q factor of a resonator is defined as $Q = \nu_0/\Delta\nu$, where ν_0 is the resonance frequency and $\Delta\nu$ stands for the linewidth of the resonance dip or peak. By fitting the measured transmission spectra with Lorentzian function, ν_0 and $\Delta\nu$ and then the corresponding Q factor were obtained. The highest Q factor of our LN WGM resonator was measured to be 1.19×10^6 as shown in Fig. 3(b). To the best of our knowledge, it is the first time that a LN resonator with Q factor higher than one million was fabricated by using microfabrication techniques allowing mass production. We noticed that the higher Q factor of our sample was usually observed in one of the two very closely neighboring WGMs as shown in Fig. 3(b). Those closely neighboring modes may originate from the mode splitting effect, which is more remarkable for a high-Q mode. The measured Q factors of 16 LN resonators on two samples produced in a batch were plotted statistically in Fig. 3(c), which shows a good reproducibility of Q factor of our resonators. Note that our processing methods and the original LNOI wafer are similar to those used by C.

#246339 Received 20 Jul 2015; revised 17 Aug 2015; accepted 18 Aug 2015; published 24 Aug 2015

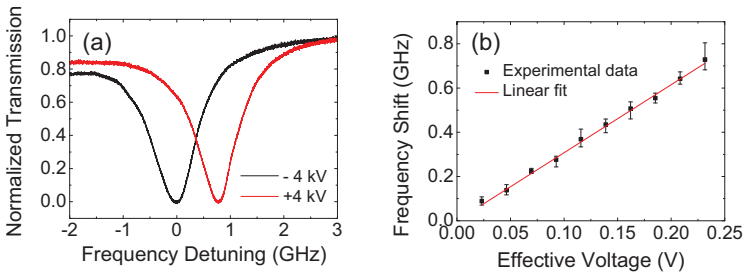

Fig. 4. Electro-optic modulation in LN resonators. (a) Normalized transmission measured when -4kV (black curve) and +4kV (red curve) voltage were applied across the parallel-plate capacitor, in which the LN chip was adhered on top of the bottom ITO glass of the capacitor. (b) The shift of resonance wavelength of the LN resonator with a radius 39.6 μm with respect to the effective voltage applied across the LN microdisk resonator. The tuning rate of resonance frequency is 3.0 GHz/V.

Wang et. al., however, the Q factors of our resonators are one order of magnitude higher than 1.02×10^5, the Q factor of their resonators [9]. We attribute the improvement in Q factors of our LN resonators to two factors: (1) A thicker LN layer providing better mode confinement. The thickness of 0.5 μm in our case is much large as compared to that of Wang's resonator (0.3 μm); (2) A smooth top surface that was untouched during the whole Ar^+ plasma etching process leading to less scattering of light.

A broad-band transmission spectrum as shown in Fig. 3(d) was recorded as well. From Fig. 3(d), the free spectrum ranges (FSR) of the modes in red, blue, green, and purple were measured to be 4.62 nm, 4.56 nm, 4.61 nm, and 4.65 nm, respectively. FSR of different kinds of eigenmodes with central wavelengths near 1550 nm in a LN microdisk resonator with a radius of 39.6 μm and a thickness of 0.5 μm were theoretically calculated by performing a full vectorial finite-element analysis [16]. In simulation, the ordinary and extraordinary refractive indices of LN crystal were set as $n_o = 2.2113$ and $n_e = 2.1377$, respectively, and no dispersion was considered because we focused on a narrow wavelength band near 1550 nm. By comparing the experimentally measured and theoretically calculated resonance wavelengths and FSR, the approximate mode numbers were assigned and labeled as (m, n) in Fig. 3(d), where m and n are mode numbers in the radial and azimuthal directions, respectively. All those observed modes were quasi-TE mode with electric field mainly in the radial direction, which experienced the extraordinary refractive index in our resonators made from a z-cut LN film.

4. Electro-optic modulation in LN resonators

It is well known that optical devices made from LN crystal allowing actively electric control [12, 17] due to the outstanding electro-optic effect of LN crystal. Herein, we demonstrated electro-optic modulations in our LN resonators by applying an external voltage perpendicular to the top surface of the LN microdisk. In the experiments, two ITO glass substrates were used as the electrodes to form a parallel-plate capacitor with a space interval of 1.1 mm. The LN chip was adhered on top of the bottom ITO glass using UV curing adhesive and thus placed inside the capacitor. An external voltage V was applied on the ITO electrodes through wires directly. Because the thickness of the LN microdisk is only 1/2200 of the distance between the two electrodes of the parallel-plate capacitor, it is necessary to apply a high voltage to the capacitor to get a significant effective voltage V_{eff} across the LN layer.

A series of transmission spectra for a LN microdisk resonator with a 39.6-μm radius were

#246339 Received 20 Jul 2015; revised 17 Aug 2015; accepted 18 Aug 2015; published 24 Aug 2015

measured when the external voltage applied across the capacitor was tuned. Two typical normalized transmission spectra, which were obtained when $V = \pm 4$ kV are shown in Fig. 4(a). The corresponding effective voltage V_{eff} applied across the LN microdisk equals to ± 0.116 V. V_{eff} was calculated by considering the system as a 1.1-mm thick parallel-plate capacitor filled in turn with 0.5-mm thick LN, 2-μm thick air, 0.5-μm thick LN, and 0.6-mm thick air. The permittivities of LN crystal and air were set as 4.57 and 1, respectively. It is clearly seen from Fig. 4(a) that the resonance frequency of the WGM in the LN resonator was shifted by 0.79 GHz when the applied voltage was changed by 8 kV. By linearly fitting the shift in the resonance frequency with respect to the effective voltage applied across the LN microdisk, we obtained a 3.0-GHz/V tuning rate of the shift of resonance frequency versus the effective voltage.

Electro-optic modulators were also successfully demonstrated in waveguide coupled microring [18], microdisk [19], and racetrack resonators [20] made from silicon. The refractive index of silicon on which the microresonators were fabricated was modulated electrically by injecting electrons and holes using p-i-n junction structures [18–20] other than linear electro-optic effect (Pockels effect). Thanks to the compact structure of the whole setup including the electrodes, the performance of the aforementioned silicon modulators are much better than our present proof-of-principle setup with two electrodes separated by 1.1 mm. The modulation frequency and driving voltage of the electro-optic modulators based on silicon microresonators were up to tens of GHz and down to 1 V [20], respectively. The performance of electro-optic modulators based on LN resonators has great potential to be improved by optimizing their structures such as the electrode structure to reduce the capacitor of the whole structure.

5. Conclusion

In summary, on-chip LN microdisk resonators with Q factors up to 1.19×10^6 were made on a LNOI wafer by using UV-lithography, Ar^+ plasma etching and HF etching techniques. It is the first time that a monocrystalline LN resonator on a chip with a Q factor higher than one million was fabricated. The fabrication techniques compatible to the conventional semiconductor processing methods allow batch manufacturing with good reproducibility. Benefiting from the large electro-optic coefficient of LN crystal and a high Q factor of our microdisk resonators, electro-optic modulation with a 3.0 GHz/V tuning rate of the shift in resonance wavelength with respect to the effective voltage applied across the LN resonator was realized. Our work helps to integrate photonic devices on a chip of LN crystal. The fabricated high-Q LN resonators have potential to be used in many applications, such as ultra-sensitive sensing [21–24] and low-threshold lasing [25], and fundamental studies ranging from PT-symmetry [26, 27] to electromagnetically induced transparency in whispering-gallery microcavities [28].

Acknowledgment

This work was financially supported by the 973 programs (Grant Nos. 2011CB922003 and 2013CB328702), the NSFC (Grant Nos. 11374165, 11174153, and 10804054), the 111 Project (Grant No. B07013).

#246339 Received 20 Jul 2015; revised 17 Aug 2015; accepted 18 Aug 2015; published 24 Aug 2015